1-1-2003

Tricarbonylrhenium(I) halide complexes of chiral non-racemic 2-(dioxolanyl)-(dioxanyl)pyridine ligands: synthesis, NMR and DFT calculations.

Peter J. Heard
Glyndwr University, p.heard@glyndwr.ac.uk

Paul M. King

Phunrawie Sroisuwan

Nikolas Kaltsoyannis

Available online at www.sciencedirect.com
SCIENCE DIRECT®
PERGAMON
Polyhedron xxx (2003) xxx–xxx
POLYHEDRON
www.elsevier.com/locate/poly

Tricarbonylrhenium(I) halide complexes of chiral non-racemic 2-(dioxolanyl)-6-(dioxanyl)pyridine ligands: synthesis, NMR and DFT calculations

Peter J. Heard [a,*], Paul M. King [a], Phunrawie Sroisuwan [a], Nikolas Kaltsoyannis [b]

[a] School of Biological and Chemical Sciences, Birkbeck University of London, Malet Street, London WC1E 7HX, UK
[b] Department of Chemistry, University College London, Christopher Ingold Laboratories, 20 Gordon Street, London WC1H 0AJ, UK

Received 2 June 2003; accepted 13 August 2003

Abstract

The chiral non-racemic O/N/O donor ligands 2-[(4*R*,5*R*)-4,5-dimethyl-1,3-dioxolan-2-yl]-6-[(4*R*,6*R*)-4,6-dimethyl-1,3-dioxan-2-yl]pyridine and 2-[(4*R*,5*R*)-4,5-dimethyl-1,3-dioxolan-2-deuteryl]-6-[(4*R*,6*R*)-4,6-dimethyl-1,3-dioxan-2-yl]pyridine were prepared in a stepwise fashion form 2,6-dibromopyridine. Reaction with the pentacarbonylhalogenorhenium(I) compounds yields the complexes $[ReX(CO)_3L]$, in which the ligands act in a N/O bidentate chelate fashion. There are eight possible diastereoisomers, three of which are observable in solution. DFT calculations indicate that the relative stability of the diastereoisomers is $SR^5 > RR^5 > SS^5 \approx RS^5 > RS^6 > SS^6 > RR^6 > SR^6$. Above ambient temperature, a dynamic process leads to the exchange of 2 of the 3 diastereoisomers: the free energy of activation is ca. 79 kJ mol^{-1}. The results of the DFT calculations and the magnitude of $\Delta G^{\ddagger}$ suggest the dynamic process to be the *flip* of the co-ordinated acetal ring.

Keywords: 6-Bromopyridine-2-aldehyde; Tricarbonylrhenium(I) halide complexes; Diastereoisomers; ^{1}H NMR

1. Introduction

Chiral non-racemic C_2-symmetric N/N/N tridentate ligands, such as 2,6-bis(oxazolinyl)pyridines have been used extensively as auxiliary ligands in both stoichiometric and catalytic transition metal-mediated enantioselective organic transformations [1]. When such ligands are restricted to a bidentate bonding mode, the ligands undergo a dynamic stereochemical rearrangement that leads to the exchange of co-ordinated and pendant donor groups [2,3]. The chiral centres on the ligands provide an excellent spectroscopic handle on the stereodynamics, allowing the fluxional pathway to be determined unambiguously.

Recently, as part of our ongoing researches on fluxionality in 'chiral-at-ligand' organo-transition metal complexes, we reported on the tricarbonylhalogenorhenium(I) complexes of the O/N/O hybrid ligands 2,6-bis[(4*R*,5*R*)-4,5-dimethyl-1,3-dioxolan-2-yl]pyridine (L^1) [4] and 2,6-bis[(4*R*,6*R*)-4,6-dimethyl-1,3-dioxan-2-yl]pyridine (L^2) [5] (Fig. 1). These complexes undergo three dynamic processes; namely a flip of the co-ordinated acetal ring and exchange of the co-ordinated and pendant acetal rings via tick-tock and rotation mechanisms [4,5]. The size of the acetal ring [five-membered (dioxolanyl) or six-membered (dioxanyl)] has opposite effects on the relative energies of ring flip and tick-tock processes: $\Delta G^{\ddagger}$ for the ring flip process is lowered on substitution of L^1 for L^2, while that for the tick-tock exchange increases. The reasons for this were not obvious and we therefore chose to investigate the analogous complexes of the mixed acetal ligand 2-[(4*R*,5*R*)-4,5-dimethyl-1,3-dioxolan-2-yl]-6-[(4*R*,6*R*)-4,6-dimethyl-1,3-dioxan-2-yl]pyridine (L^{HH}) in an attempt to gain further insights on the problem. The results of this study are reported here.

* Corresponding author. Tel.: +44-20-7679-7480; fax: +40-20-7679-7464.
E-mail address: p.heard@bbk.ac.uk (P.J. Heard).

0277-5387/$ - see front matter © 2003 Published by Elsevier Ltd.
doi:10.1016/j.poly.2003.08.012

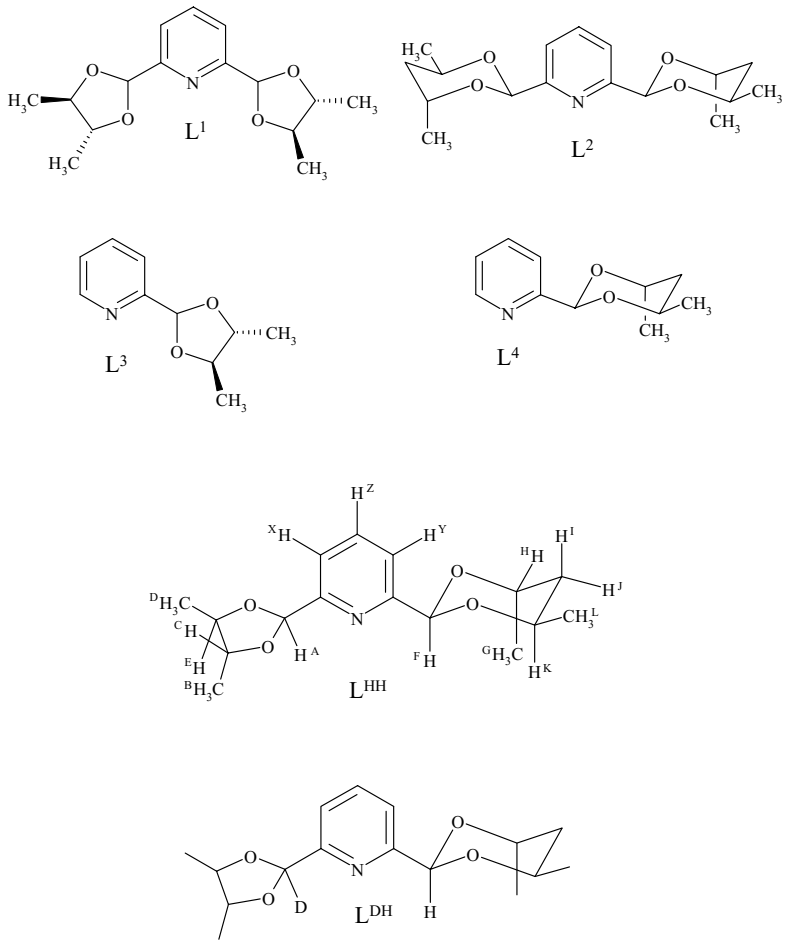

Fig. 1. The chrial non-racemic ligands L^1, L^2, L^3, L^4, L^{HH} and L^{HD}, showing the hydrogen atom labelling for L^{HH}.

2. Results

2.1. The ligands

2-[(4*R*,5*R*)-4,5-dimethyl-1,3-dioxolan-2-yl]-6-[(4*R*,6*R*)-4,6-dimethyl-1,3-dioxan-2-yl]Pyridine (L^{HH}) was synthesised from 2,6-dibromopyridine, as shown in Scheme 1, and characterised by mass spectrometry and NMR: data are reported in Tables 1 and 2. Both routes give similar overall yields. During the work-up of (**3a**/**3b**), the attached acetal ring can be cleaved by hydrochloric acid, used in the work-up, yielding a small amount of 2,6-pyridinedicarboxaldehyde. Route (i) is thus the preferred pathway: (2*R*,3*R*)-butane-2,3-diol is the cheaper of the diols.

The ^{1}H NMR spectrum of L^{HH} is fully and unambiguously assignable. The acetal-C hydrogens, H_A (dioxolanyl) and H_F (dioxanyl) (see Fig. 1 for hydrogen atom labelling), are identified by their low frequency shifts (ca. δ 6.0) and differentiated by a NOESY experiment. H_A undergoes cross-relaxation with Me_B and H_E, which are assigned to the dioxolanyl ring on the basis of their scalar couplings, while H_F undergoes cross-relaxation with H_L and Me_G, of the dioxanyl ring. The NOEs observed between H_F and H_L, and H_F and Me_G are consistent with the dioxanyl ring adopting a chair configuration with the pyridine ring equatorial. The full AB_3CD_3E and AB_3CDEFG_3 spin systems of the dioxolanyl and dioxanyl rings were analysed (non-iteratively) using the program GNMR [6]. The 3- and 5-position hydrogens of the pyridine ring, H_X and H_Z, are distinguished by virtue of the fact that they undergo cross-relaxation with the acetal-C hydrogens, H_A and H_F, respectively. The ^{13}C NMR spectrum was assigned on the basis of signal chemical shifts, DEPT experiments and by comparison with the spectra obtained [7] for L^1, L^2, 2-[(4*R*,5*R*)-4,5-dimethyl-1,3-dioxolan-2-yl]pyridine (L^3) [8] and 2-[(4*R*,6*R*)-4,6-dimethyl-1,3-dioxan-2-yl] pyridine (L^4) [5]. NMR data are reported in Table 2.

The deuterium labelled analogues of L^{HH}, namely 2-[(4*R*,5*R*)-4,5-dimethyl-1,3-dioxolan-2-deuteryl]-6-[(4*R*,6*R*)-4,6-dimethyl-1,3-dioxan-2-yl]pyridine (L^{DH}) and 2-[(4*R*,5*R*)-4,5-dimethyl-1,3-dioxolan-2-deuteryl]-6-[(4*R*,6*R*)-4,6-dimethyl-1,3-dioxan-2-deuteryl]pyridine (L^{DD}) were prepared similarly, using d_7-dimethylformamide in the

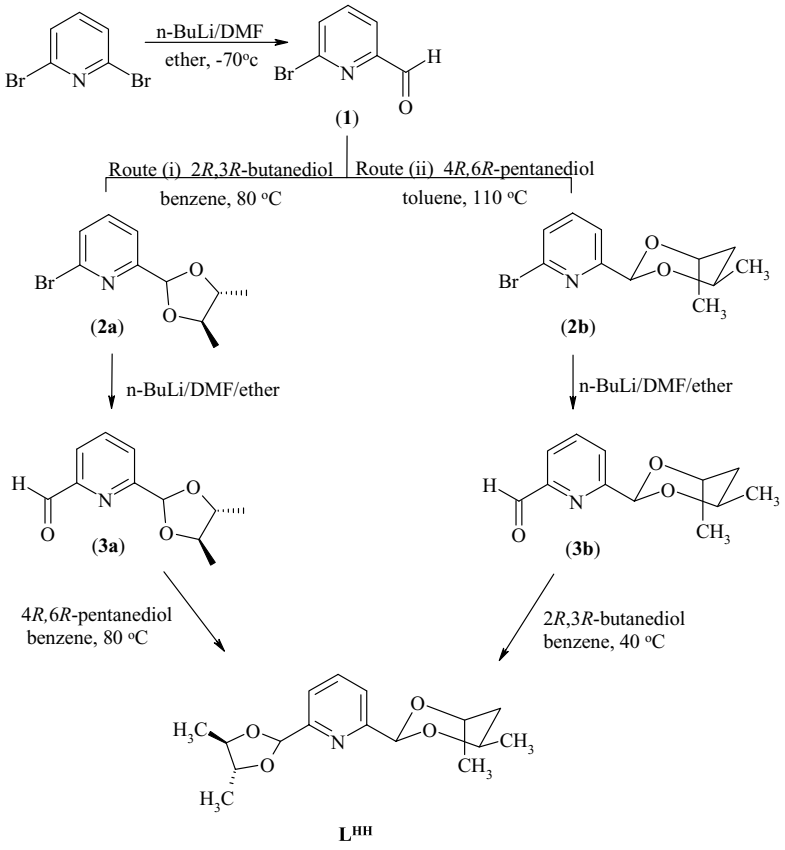

Scheme 1.

appropriate step(s) (Scheme 1), and identified by mass spectrometry and NMR: data are reported in Tables 1 and 2. The selective deuteration of the dioxolanyl ring (synthesis of L^{DH}) is best achieved by reaction of 2-deuteraldehyde-6-[(4*R*,6*R*)-4,6-dimethyl-1,3-dioxan-2-deuteryl]pyridine with (2*R*,3*R*)-butane-2,3-diol [i.e., route (ii), Scheme 1]. This route gives the best overall yield of L^{DH} and minimises the amount of 2-[(4*R*,5*R*)-4,5-dimethyl-1,3-dioxolan-2-yl]-6-[(4*R*,6*R*)-4,6-dimethyl-1,3-dioxan-2-deuteryl]pyridine (L^{HD}), which is produced as a side product: careful control of the reaction conditions enabled L^{DH} to be isolated in 80% excess over

Table 1
Analytical data for L^{HH}, L^{DH} and L^{DD}, and the complexes $[ReX(CO)_3(L)]$ (L = L^{HH}, X = Cl, Br or I) and $[ReBr(CO)_3(L^{HD})]$

Ligand/Complex	Reaction time (h)	Yield (%)	ν(CO)[a] (cm^{-1})	Mass spectral data	Analyses[b] (%)		
					C	H	N
L^{HH}				316 $[M + Na]^+$ 294 $[M + H]^+$			
L^{DH}				317 $[M + Na]^+$ 295 $[M + H]^+$			
L^{DD}				318 $[M + Na]^+$ 296 $[M + H]^+$			
$[ReCl(CO)_3(L^{HH})]$	24	79	1904; 1917; 2031	599 $[M]^+$ 564 $[M - Cl]^+$	37.24 (38.09)	3.72 (3.87)	2.18 (2.34)
$[ReBr(CO)_3(L^{HH})]$	72	62	1905; 1919; 2031	643 $[M]^+$ 564 $[M - Br]^+$	36.65 (35.46)	3.64 (3.60)	2.39 (2.18)
$[ReI(CO)_3(L^{HH})]$	96	68	1909; 1920; 2031	691 $[M]^+$ 564 $[M - I]^+$	34.57 (33.05)	3.53 (3.36)	2.32 (2.03)
$[ReBr(CO)_3(L^{DH})]$	72	51	1906; 1919; 2031	644 $[M]^+$ 565 $[M - Br]^+$	32.94 (35.41)	3.41 (3.44)	1.85 (2.17)

Yield reported relative to the $[ReX(CO)_5]$ compounds.
[a] Infrared data. Spectra recorded in CH_2Cl_2 solution.
[b] Calculated values in parentheses. Poor analytical figures due to impurities, which could not be separated (see text).

Table 2
NMR data[a] L^{HH}

Assignment[b]	^{1}H NMR data		Assignment	^{13}C NMR data
	δ	Scalar couplings (Hz)		δ
H_A	6.01 (6.0)[b]		CH_3	16.9
H_B	1.34	J_{BC} 6.1; J_{BE} 0.1	CH_3	17.0
H_C	3.80	J_{CD} 0.1; J_{CE} 7.6	CH_3	17.3
H_D	1.38	J_{DE} 6.1	CH_3	21.9
H_E	3.84		CH_2	36.8
H_F	5.95 (5.9)[c]		$CHCH_3$ (dioxanyl ring)	68.1
H_G	1.50	J_{GH} 6.9	$CHCH_3$ (dioxanyl ring)	68.8
H_H	4.49	J_{HI} 6.1; J_{HJ} 1.0	$CHCH_3$ (dioxolanyl ring)	78.8
H_I	2.02	J_{IJ} 13.3; J_{IK} 11.7	$CHCH_3$ (dioxolanyl ring)	80.4
H_J	1.45	J_{JK} 2.4	acetal-*C* (dioxanyl ring)	94.8 (25)[d]
H_K	4.24	J_{KL} 6.2	acetal-*C* (dioxolanyl ring)	102.0 (25)[e]
H_L	1.27		pyridine-C	120.3; 121.2; 137.7; 156.7[f]; 157.3[f]
H_X	7.79			
H_Y	7.66	J_{XY} 7.8; J_{XZ} 7.7		
H_Z	7.58	J_{YZ} 1.1		

[a] Recorded in $CDCl_3$ at 298 K; chemical shifts quoted relative to trimethylsilane. See Fig. 1 for assignments.
[b] δ ^{2}H for L^{DH}/L^{DD} given in parentheses.
[c] δ ^{2}H L^{DD} given in parentheses.
[d] $^1J_{CD}$/Hz for L^{DH}/L^{DD} given in parentheses.
[e] $^1J_{CD}$/Hz for L^{DD} given in parentheses.
[f] Quaternary carbon.

L^{HD}. Attempts to prepare L^{HD} were less successful: L^{HD} could not be prepared cleanly.

2.2. Complexes

The complexes, $[ReX(CO)_3L]$ ($L = L^{HH}$, $X = Cl$, Br or I; $L = L^{DH}$, $X = Br$) were prepared by refluxing the $[ReX(CO)_5]$ compounds with a small excess of the appropriate ligand in chloroform. The complexes were isolated as air-stable, microcrystalline solids, soluble in common organic solvents. The infrared spectra of the complexes each displayed three bands in the carbonyl stretching region, characteristic of a *fac*-octahedral co-ordination geometry for the $[Re(CO)_3]$ moiety [9], indicating the potentially terdenate ligands are binding in the expected N/O bidentate fashion. The FAB mass spectra of the complexes each display low intensity peaks due to the molecular ions, $[M]^+$, and high intensity peaks due to the species $[M - \text{halogen}]^+$. The poor analytical figures obtained, particularly for $[ReBr(CO)_3L^{DH}]$, result from the presence of impurities, which are evidenced in the NMR spectra. Analytical data are reported in Table 1.

Assuming that inversion of configuration at the co-ordinated oxygen atom is rapid [10], the $[ReX(CO)_3L]$ ($L = L^{HH}$ or L^{DH}) complexes possess six chiral centres: the 4- and 5-positions of the dioxolanyl ring, the 4- and 6-positions of the dioxanyl ring, the acetal-carbon atom of co-ordinated acetal ring, and the metal centre. The configuration at 4- and 5-, and 4- and 6-acetal ring positions are fixed (R), but the configurations at the acetal-carbon and the metal can be R or S. Thus, there are eight possible diastereoisomers, namely RR^5, RS^5, SR^5, SS^5, RR^6, RS^6, SR^6 and SS^6, depending on the configuration at the metal and at the co-ordinated acetal-carbon, respectively. The numbers refer to which acetal ring [dioxolanyl (5) or dioxanyl (6)] is co-ordinated (Fig. 2). The configuration at the metal is defined by viewing the metal down the pseudo C_3 axis of symmetry, with the three CO groups down, and assigning priorities to the three remaining ligands according to the Cahn–Ingold–Prelog system [11].

The ambient temperature solution ^{1}H NMR spectra of the $[ReX(CO)_3L^{HH}]$ complexes are highly complex due to the overlapping sub-spectra of at least 3 of the 8 possible diastereoisomers (although exchange is slow on the NMR time scale, the diastereoisomers interconvert in solution, frustrating attempts to separate them [4,5,8]). The acetal-CH region, which is most amenable to analysis, displays three pairs of singlets; each diastereoisomer gives rise to two acetal-CH signals. Additional weak signals that may be due to the presence of minor diastereoisomers or impurities are also observed. The intensities of these additional signals vary, depending on the reaction conditions and the method of purification, suggesting they are more likely to be due to impurities. The assignment of the acetal-CH signals to the dioxolanyl and dioxanyl rings was done on the basis of their spin–lattice relaxation times. Extensive T_1 measurements [7] on ligands L^1–L^4 and their tricarbonylhalogenorhenium(I) complexes indicate

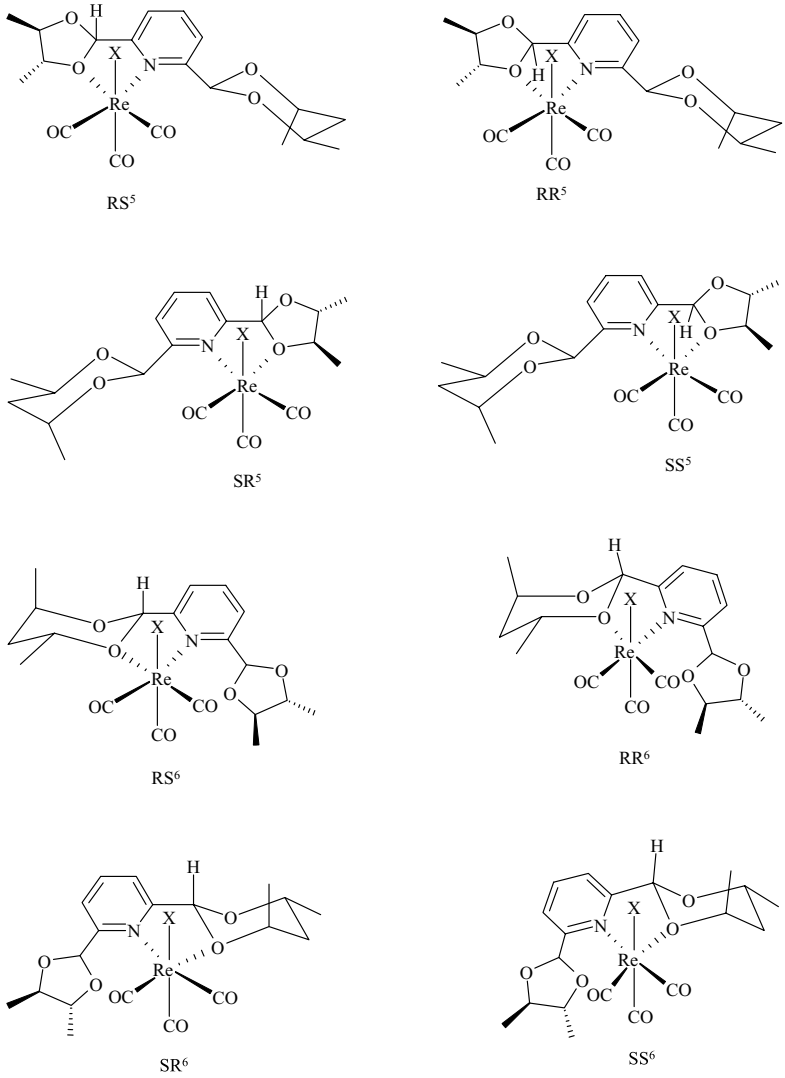

Fig. 2. The eight possible diastereoisomers of the complexes [ReX(CO)$_3$L] X = Cl, Br or I; L = L^{HH} or L^{DH}). Letters refer to the configuration at the metal and at the acetal-carbon atom of the co-ordinated ring.

that the relaxation times for the dioxolanyl-CH's are between ca. 2.4 and 3.2 s, while those for the dioxanyl-CH are between ca. 1.0 and 1.5 s; as might be expected, the relaxation times in the free ligands are generally longer then those in the complexed ligands. The relaxation times of H_A (dioxolanyl) and H_F (dioxanyl) of free L^{HH} are ca. 2.5 and 1.0 s, respectively. The pairs of acetal-CH signals in the [ReX(CO)$_3$L^{HH}] complexes also possess T_1 values of ca. 2.5 and 1.0 s (Table 3) and are thus assigned to the dioxolanyl and dioxanyl rings, respectively. The ^{1}H NMR spectrum of [ReBr(CO)$_3$L^{DH}] confirms the assignment. The sub-spectra due to the acetal-ring- and pyridine-hydrogens are also consistent with the presence of three main diastereoisomers, but the extensive overlap of signals frustrated attempts to analyse the spectra fully in these regions. ^{1}H NMR data for the acetal-C hydrogens are reported in Table 3.

It is not possible to determine which of the eight possible diastereoisomers are observed in solution from the NMR spectra. Quantum chemical (DFT) calculations (Table 4) show clearly that co-ordination of the dioxolanyl ring is favoured strongly over the dioxanyl ring. The relative stabilities of the diastereoisomers are in the order $SR^5 > RR^5 > SS^5 \approx RS^5 > RS^6 > SS^6 > RR^6 > SR^6$, suggesting that the three solution-state species are SR^5, RR^5 and either SS^5 or RS^5. This is in accord with trends observed previously in the complexes [ReX(CO)$_3$L^1] (SR > RR > SS > RS) [4] and [ReX(CO)$_3$L^3] (SR > RR > RS > SS) [8]. The reasons for the calculated trend are not obvious; however, the amount by which the ligand is destabilised on binding appears to at least play a role. Single point energy calculations were performed on the ligand in each of its bound geometries (the geometry being that taken from the DFT optimisations) and compared to that of the free

Table 3
^{1}H NMR data[a] for the [ReX(CO)$_3$(L)] (L = L^{HH}, X = Cl, Br or I; L = L^{DH}, X = Br) complexes

Compound	Diastereoisomer[b]	δ(acetal-CH)[c]	
		H_A	H_F
[ReCl(CO)$_3$ (L^{HH})]	**A** (60)	6.37 (2.6)	6.55 (1.1)
	B (34)	6.81 (2.4)	6.45 (1.2)
	C (6)	6.62[f]	6.10 (1.2)
[ReBr(CO)$_3$(L^{HH})]	**A** (54)	6.37 (2.6)	6.51 (1.0)
	B (43)	6.83 (2.4)	6.43 (1.2)
	C (3)	6.57[d]	6.08 (1.2)
[ReI(CO)$_3$(L^{HH})]	**A** (64)	6.34 (2.4)	6.40 (1.0)
	B (26)	6.76 (2.4)	6.38 (1.2)
	C (10)	6.57 (2.5)	6.05 (1.2)
[ReBr(CO)$_3$(L^{DH})]	**A** (60)		6.51 (1.0)
	B (32)		6.43 (1.2)
	C (8)		6.08 (1.2)

[a] Recorded in $CDCl_3$ solution at 298 K; chemical shifts quoted relative to tetramethylsilane.
[b] Populations (%) given in parentheses.
[c] Spin lattice relaxation times, measured at 273 K, given in parentheses.
[d] T_1 not measured due to overlap signals arising from minor impurities.

Table 4
Calculated energies for the complex [ReCl(CO)$_3$L^{HH}]

Diastereoisomer[a]	E_{rel}[b] (kJ mol^{-1})
SR^5	0
RR^5	9
SS^5	15
RS^5	15
RS^6	28
SS^6	32
RR^6	39
SR^6	50

[a] See Fig. 2 for labelling.
[b] Relative energy.

ligand. The results (Table 5) indicate that the ligand is destabilised on binding; the amount by which the ligand is destabilised follows the trend SR^5 < RR^5 < RS^5 < SS^5 < RS^6 ≈ SS^6 < RR^6 < SR^6, close to the trend in the relative energies of the complexes (see above).

Table 5
Calculated energies for isolated ligand, L^{HH}

Ligand geometry[a]	E_{rel}[b] (kJ mol^{-1})
Free ligand	0
SR^5	33
RR^5	37
RS^5	40
SS^5	41
RS^6	45
SS^6	45
RR^6	49
SR^6	58

[a] Labels refer to the diastereoisomer in which a particular geometry occurs (see text). See Fig. 2 for labelling.
[b] Relative energy.

On warming, the ^{1}H NMR signals display reversible band broadening, due to a dynamic process that leads to the interconversion of diastereoisomers (**B**) and (**C**) (see Table 2 for labelling). There are three possible exchange pathways, namely a flip of the co-ordinated acetal ring, the tick-tock exchange of pendant and co-ordinated acetal rings and the rotational exchange of pendant and co-ordinated acetal rings [4,5,8]. Although these pathways are distinguishable by their different effects on the NMR lineshapes in the intermediate exchange regime, the uncertainty in the spectral assignment frustrated a full and unambiguous analysis of the spin problem. The barrier for the exchange process was estimated from selective inversion experiments, and found to be ca. 79 kJ mol^{-1} (there is no significant halogen dependence). For either the tick-tock or rotation processes to be observed, at least one Re-dioxanyl species would need to be evidenced in the NMR spectrum, which the DFT calculations indicate to be unlikely (see above). The dynamic process was therefore assigned tentatively to the acetal ring flip fluxion: the energy barrier measured is close to that observed for the ring flip fluxion in the analogous complexes of L^1 (Table 6).

Table 6
Summary of fluxional energetics in the complexes [ReX(CO)$_3$L] (X = Cl, Br or I; L = L^1, L^2, L^3 or L^4)[a]

Halide	$\Delta G^{\ddagger}$ (acetal ring flip) (kJ mol^{-1})				$\Delta G^{\ddagger}$ (tick-tock exchange) (kJ mol^{-1})			
	[ReX(CO)$_3$L^1]	[ReX(CO)$_3$L^3]	[ReX(CO)$_3$L^2]	[ReX(CO)$_3$L^4]	[ReX(CO)$_3$L^1]	[ReX(CO)$_3$L^3]	[ReX(CO)$_3$L^2]	[ReX(CO)$_3$L^4]
Chloride	77	88	[b]	82	72	[c]	79	[c]
	[b]	84	[b]	81	[b]	[c]	[b]	[c]
Bromide	77	87	[b]	81	72	[c]	77	[c]
	[b]	86	[b]	81	[b]	[c]	[b]	[c]
Iodide	78	85	[b]	78	73	[c]	75	[c]
	[b]	[b]	[b]	81	[b]	[c]	[b]	[c]

[a] Data published in [4,5] and [8].
[b] Not all fluxional processes are measurable due to the different diastereoisomer populations.
[c] The tick-tock fluxion does not occur in complexes of L^3 or L^4.

3. Discussion

Table 6 summarises the activation energies for the acetal-ring flip and tick-tock exchange processes in the tricarbonylhalogenorhenium(I) complexes of L^1–L^4. Data show that substitution of the dioxolanyl ligands with the dioxanyl ligands has opposite effects on the energy barriers: $\Delta G^{\ddagger}$ (ring flip) decreases, while $\Delta G^{\ddagger}$ (tick-tock) increases. This observation was difficult to rationalise and led to the study reported here. It was believed initially [5] that the ground-state energy was lower in the dioxanyl complexes. The DFT calculations indicate clearly that this is not the case: binding of dioxolanyl ring in $[ReX(CO)_3L^{HH}]$ is favoured by ca. 12–50 kJ mol^{-1}. The lower ground state energy in the dioxolanyl complexes presumably accounts for the increased barrier to the ring flip process.

The lower ground state energy of the dioxolanyl complexes may also be expected to result in an increase in the barrier to the tick-tock exchange fluxion, which is not the case. Thus the decrease in the barrier to the tick-tock exchange fluxion that occurs when L^2 is substituted with L^1 must be the result of a greater stabilisation of the transition state energy. This stabilisation arises presumably because of the more favourable Re-dioxolanyl interactions in the transition state, in which the ligand is bound to the metal centre in a pseudo-terdentate fashion [4,5].

4. Experimental

4.1. Synthetic methods

All procedures were carried out using standard Schlenk techniques under an atmosphere of dry, oxygen-free nitrogen. Solvents were dried by distillation from appropriate drying agents [12] and stored under nitrogen. Starting materials were purchased from standard sources. The $[ReX(CO)_5]$ (X = Cl, Br or I) compounds were prepared by previously published procedures [13].

The non-racemic chiral acetal ligand 2-[(4*R*,5*R*)-4,5-dimethyl-1,3-dioxolan-2-yl]-6-[(4*R*,6*R*)-4,6-dimethyl-1,3-dioxan-2-yl]pyridine (L^{HH}) was synthesised in a stepwise fashion from 2,6-dibromopyridine, as detailed below. L^{HH} can be prepared via either route (i) or route (ii) (Scheme 1). The former pathway is the economically preferred route because, during preparation of (**3a**) or (**3b**), the acetal group reacts with hydrochloric acid, which is used in the work-up, to yield 2,6-pyridinedicarboxaldehyde: (4*R*,6*R*)-pentanediol is the more expensive diol.

4.1.1. 6-Bromopyridine-2-aldehyde (**1**)

6-Bromopyridine-2-aldehyde was prepared using a procedure adapted from that previously published [14]. To a slurry of 10.0 g (0.042 mol) of 2,6-dibromopyridine in 250 cm^3 of cold (−80 °C) diethyl ether, 27.0 cm^3 of 1.6 M of *n*-butyllithium in hexanes was added dropwise. After the addition was complete, the reaction mixture was allowed to warm to −40 °C; a clear yellow solution resulted. This solution was cooled to −80 °C and 7 cm^3 (0.084 mol) of *N*,*N*-dimethylformamide in diethyl ether (20 cm^3) was added slowly. The reaction was stirred at −70 °C for 2 h, during which time a white solid precipitated. The mixture was allowed to warm to −10 °C and hydrolysed with 10 cm^3 of concentrated hydrochloric acid. The aqueous phase was separated and extracted with diethyl ether. The extracts and ether phase were combined, washed with water, dried over magnesium sulfate, and evaporated to dryness. Crystallisation of the solid residue from a diethyl ether/*n*-pentane mixture gave 5.94 g (76%) of pure (**1**).

4.1.2. 2-[(4R,5R)-dimethyl-1,3-dioxolan-2-yl]-6-Bromopyridine (**2a**)

1 (5.0 g, 0.027 mol), (2*R*,3*R*)-butanediol (2.7 cm^3, 0.030 mol), 2,2-dimethoxypropane (3.7 cm^3, 0.030 mol), and *para*-toluenesulfonic acid (ca. 100 mg) were refluxed for 18 h in 30 cm^3 of benzene. The resulting solution was extracted with aqueous sodium carbonate solution (3×30 cm^3) then water (3×30 cm^3), dried over magnesium sulfate, and concentrated to dryness in vacuo. The solid residue was crystallised from hot hexane, yielding pure (**2a**). Yield: 3.6 g (52%).

4.1.3. 2-[(4R,5R)-dimethyl-1,3-dioxolan-2-yl]-6-Aldehydepyridine (**3a**)

2-[(4*R*,5*R*)-dimethyl-1,3-dioxolan-2-yl]-6-Aldehydepyridine was prepared using a similar procedure to that for (**1**). Yield: 38%.

4.1.4. 2-[(4R,5R)-dimethyl-1,3-dioxolan-2-yl]-6-[(4R,6R)-4,6-dimethyl-1,3-dioxan-2-yl]Pyridine (L^{HH})

3a (0.80 g, 3.86 mmol), (4*R*,6*R*)-pentanediol (0.41 g, 3.90 mmol), 2,2-dimethoxypropane (0.48 cm^3, 3.90 mmol), and *para*-toluenesulfonic acid (ca. 100 mg) were refluxed for 72 h in 30 cm^3 of toluene. The resulting solution was extracted with aqueous sodium carbonate solution (3×30 cm^3) then water (3×30 cm^3), dried over magnesium sulfate, and concentrated to dryness in vacuo. The residue was crystallisation from hot petroleum ether to yield 0.71 g (63%) of L^{HH}.

4.2. Physical methods

^{1}H, ^{13}C and ^{2}H NMR spectra were recorded on a Bruker DRX500 Fourier transform spectrometer operating at 500.13, 125.75 and 76.77 MHz, respectively. Chemical shifts are quoted relative to tetramethylsilane. Probe temperatures were controlled by a standard B-VT

2000 unit and are considered accurate to ±1 K. Spin–lattice relaxation times, and COSY and NOESY spectra were obtained using the standard Bruker automation programs T1IR, COSYST and NOESYST, respectively. Selective inversion experiments were carried out using our SOFTPULVD program, which generates the pulse sequence D1-180°-REBURP55-VD-90°-FID. The relaxation delay was 25 s and the VD list typically contained 20 delays. Exchange rates were extracted from the longitudinal magnetisations using the program CIFIT [15].

Infrared spectra were recorded in CH_2Cl_2 solution on a Shimadzu hyper 8700 FT-IR spectrometer operating in the region 4000–400 cm^{-1}. Fast atom bombardment mass spectra were obtained at the London School of Pharmacy on a VG Analytical ZAB-SE4F instrument, using Xe^+ bombardment at 8 kV energy, on samples in a matrix of 3-nitrobenzyl alcohol. Elemental analyses were carried out at University College London.

4.3. Computations

The initial free ligand geometric structure was constructed using the Molden molecular modelling software [16] using fragments taken from the Cambridge Crystallographic Database. A DFT/B3LYP [17] geometry optimisation was performed, without symmetry constraints (6-31G** basis set), using GAMESS-UK version 6.2 [18]. In order to check the conformational stability of the ligands when bound to the metal centre a number of additional calculations were performed. These compared the geometry of the bound ligand (see below) to that of the optimised free ligand. Calculations were again performed with GAMESS-UK using a 6-31G** basis-set at the DFT/B3LYP level of theory.

Calculations on the complexes were performed using the Amsterdam Density Functional program suite [19–23]. An uncontracted double-zeta Slater-type orbital valence basis set, supplemented with a p function for hydrogen and a d polarisation function for carbon, nitrogen, oxygen and chlorine (ADF Type III), was employed for the non-metallic elements. For Re, the ADF Type IV basis set, which may be described as triple-zeta without polarisation functions was used. Scalar relativistic corrections [24] were included via the ZORA to the Dirac equation [25,26]. The frozen core approximation was employed. The relativistic frozen cores (calculated by the ADF auxiliary program Dirac) used were: carbon (1s), nitrogen (1s), oxygen (1s), chlorine (2p) and rhenium (4f). The local density parameterisation of Vosko et al. [27] was employed, in conjunction with Becke's gradient correction [28] to the exchange part of the potential and the correlation correction of Perdew [29]. The default integration parameter of 4.0 was used in all calculations. Geometry optimisations were conducted without symmetry constraints, using a gradient convergence criterion of 0.005 au/Å.

Acknowledgements

We are grateful to The Royal Thai Government for a studentship (P.S.) and to Johnson Matthey for the loan of rhenium.

References

[1] A.H. Ghosh, P. Mathivanan, J. Cappiello, Tetrahedron Asymmetr. 9 (1998) 1.
[2] P.J. Heard, C. Jones, J. Chem. Soc., Dalton Trans. (1997) 1083.
[3] P.J. Heard, D.A. Tocher, J. Chem. Soc., Dalton Trans. (1998) 2169.
[4] P.J. Heard, A.D. Bain, P. Hazendonk, D.A. Tocher, J. Chem. Soc., Dalton Trans. (1999) 4495.
[5] P.J. Heard, P.M. King, D.A. Tocher, J. Chem. Soc., Dalton Trans. (2000) 1769.
[6] gNMR v4.1.0, Cherwell Scientific Limited, Oxford, 2000.
[7] P. Sroisuwan, PhD Thesis, University of London, 2002.
[8] P.J. Heard, A.D. Bain, P. Hazendonk, Can. J. Chem. 77 (1999) 1707.
[9] D.A. Edwards, J. Marshalsea, J. Organomet. Chem. 131 (1977) 73.
[10] R.F.W. Bader, J.R. Cheeseman, K.E. Laidig, K.B. Wiberg, C. Breneman, J. Am. Chem. Soc. 112 (1990) 6530.
[11] E.L. Eliel, S.H. Wilen, Stereochemistry of Organic Compounds, Wiley, New York, 1994.
[12] D.D. Perrin, W.L.F. Armarego, Purification of Laboratory Chemicals, Pergamon, Oxford, 1988.
[13] P. Schmidt, W.C. Trogler, F. Basolo, Inorg. Synth. 28 (1979) 160.
[14] J.E. Parks, B.E. Wagner, R.H. Holm, Inorg. Chem. 10 (1971) 2472.
[15] A.D. Bain, J.A. Cramer, J. Magn. Reson. A 118 (1996) 21.
[16] G. Schaftenaar, J.H. Noordik, Molden: a pre- and post-processing program for molecular and electronic structures, J. Comput.-Aided Mol. Des. 14 (2000) 123.
[17] A.D. Becke, J. Chem. Phys. 98 (1993) 5648.
[18] GAMESS-UK version 6.2, CFS Ltd., CCLRC Daresbury Laboratory, 1999. GAMESS-UK is a package of ab initio programs by M.F. Guest, J.H. van Lenthe, J. Kendrick, K. Schoffel and P. Sherwood, with contributions from R.D. Amos, R.J. Buenker, H.J.J. van Dam, M. Dupuis, N.C. Handy, I.H. Hillier, P.J. Knowles, V. Bonacic-Koutecky, W. von Niessen, R.J. Harrison, A.P. Rendell, V.R. Saunders, A.J. Stone and A.H. de Vries. The package is derived from the original GAMESS code of M. Dupuis, D. Spangler and J. Wendoloski, NRCC Software Catalog, vol. 1, Program No. QG01 (GAMESS), 1980.
[19] ADF2000, Department of Theoretical Chemistry, Vrije Universiteit, Amsterdam, 2000.
[20] E.J. Baerends, D.E. Ellis, P. Ros, Chem. Phys. 2 (1973) 41.
[21] L. Versluis, T. Ziegler, J. Chem. Phys. 88 (1988) 322.
[22] G. te Velde, E.J. Baerends, J. Comp. Phys. 99 (1992) 84.
[23] C. Fonseca Guerra, J.G. Snijders, G. te Velde, E.J. Baerends, Theor. Chem. Acc. 99 (1998) 391.
[24] N. Kaltsoyannis, J. Chem. Soc., Dalton Trans. (1997) 1.
[25] E. van Lenthe, R. van Leeuwen, E.J. Baerends, J.G. Snijders, Int. J. Quantum Chem. 57 (1996) 281.
[26] E. van Lenthe, J.G. Snijders, E.J. Baerends, J. Chem. Phys. 105 (1996) 6505.
[27] S.H. Vosko, L. Wilk, M. Nusair, Can. J. Phys. 58 (1980) 1200.
[28] A.D. Becke, Phys. Rev. A 38 (1988) 3098.
[29] J.P. Perdew, Phys. Rev. B 33 (1986) 8822.